

Experimental study on discretely modulated continuous-variable quantum key distribution

Yong Shen,¹ Hongxin Zou,^{1,*} Liang Tian,^{1,2} Pingxing Chen,¹ and Jianmin Yuan¹

¹*Department of Physics, The National University of Defense Technology, Changsha 410073, PR China*

²*College of Optoelectronic Science and Engineering, The National University of Defense Technology, Changsha 410073, PR China*

We present a discretely modulated continuous-variable quantum key distribution system in free space by using strong coherent states. The amplitude noise in the laser source is suppressed to the shot-noise limit by using a mode cleaner combined with a frequency shift technique. Also, it is proven that the phase noise in the source has no impact on the final secret key rate. In order to increase the encoding rate, we use broadband homodyne detectors and the no-switching protocol. In a realistic model, we establish a secret key rate of 46.8 kbits/s against collective attacks at an encoding rate of 10 MHz for a 90% channel loss when the modulation variance is optimal.

PACS numbers: 03.67.Dd, 42.50.-p, 89.70.+c

I. INTRODUCTION

Continuous-variable quantum key distribution (CV-QKD) by using coherent states [1] was introduced as an alternative to the single-photon-based discrete quantum key distribution (QKD) protocol [2]. In this protocol, two legitimate users (Alice and Bob) use coherent states whose X and P quadratures are Gaussian modulated to establish a shared secret key. CV-QKD has made great achievements during the past few years. At first, it was thought that no secret key rate could be obtained when the channel loss was larger than 3 dB, subsequently, the 3-dB loss limit was beaten by the methods of reverse reconciliation [3] and was experimentally demonstrated [4]. At the same time, another method called postselection [5] was proposed, which can also beat the 3-dB loss limit. Just like the discrete QKD protocol, at first, it was believed that the security of CV-QKD was based on the random switching of bases that Bob measures. Subsequently, it was found that, without switching, CV-QKD is also secure [6], and has performed experimental demonstrations [7, 8]. Several experiments of Gaussian-modulated CV-QKD with optical fibers have been implemented [9–11]. However, the distance between Alice and Bob is much shorter than that in the discrete QKD because the reconciliation efficiency of continuous variables is much lower than that of discrete variables when the signal-to-noise ratio (SNR) is small.

In order to adapt CV-QKD for long-distance communication, two CV-QKD protocols with discrete modulation were proposed [12, 13], and the former was recently experimentally implemented [14]. In these schemes, instead of Gaussian modulation, Alice modulates the quadratures of coherent states discretely. In the former protocol, Eve's attacks were restricted by tomography performed by Bob, whereas the latter offered unconditional proofs with no assumption. The security of the latter scheme is guaranteed by the optimality of Gaussian attacks [15, 16], that is, when the covariance matrix of the state shared by Alice and Bob is the same as in the Gaussian modulated case, the secret key rate is also the same.

However, discretely modulated CV-QKD is secure only when the modulation variance is small. So the SNR in discretely modulated CV-QKD is much smaller than that of the Gaussian modulated CV-QKD experiments so far, which means that the noise is more fatal in discretely modulated CV-QKD. The noise in CV-QKD mainly consists of two parts, quantum noise and classical noise. The former is induced by channel loss and can not be suppressed; the latter is called excess noise and can be arbitrarily suppressed in principle.

In this paper, we present an experimental implementation of discretely modulated CV-QKD described in Ref. [13] in free space. In order to increase the bandwidth of cryptography and to remove the noise caused by imprecise control of the relative phase between the signal and the local oscillator (LO), we use the no-switching protocol [6] instead of randomly switching the quadrature that Bob measures. Unlike Ref. [14], we use strong coherent states instead of weak coherent states for obtaining a sizable feedback signal to lock the relative phase. Additionally, the amplitude noise in the laser source is suppressed at the shot-noise limit by using a mode cleaner combined with a frequency shift technique. Also, it is proven that the phase noise in the source has no impact on the final secret key rate. As a result, we establish a secret key rate of 46.8 kbits/s for a 90% lossy channel (which corresponds to a 50 km standard telecom fiber with a 0.2-dB/km loss) under the realistic model [4].

II. THEORETICAL EVALUATION OF THE SECRET KEY RATES

A. PROTOCOL DESCRIPTION

In this section, we detail the calculation of the security bound of discretely modulated CV-QKD under collective attacks by considering the noise in the laser source.

When the noise in the source is not considered, the protocol runs as follows [13]. (i) Alice prepares one of the four coherent states: $|\alpha_k\rangle = |\alpha e^{i(2k+1)\pi/4}\rangle$ with $k \in \{0, 1, 2, 3\}$ and sends it to Bob. The real number α is chosen so as to maximize the secret key rate. (ii) When Bob receives the state, he uses a 50:50 beamsplitter to split the state into two beams. Then he

*Electronic address: hxzou@nudt.edu.cn

measures the X quadrature of one beam and the P quadrature of the other. (iii) The signal of the modulated and measured value encodes the bit of the raw key, so after Bob's measurement, he and Alice share correlated strings of bits. By reconciliation and privacy amplification they can achieve secret key. This is the *prepare and measure* version of the protocol. It is easy to implement experimentally in this version, but difficult to analyze theoretically. Usually the security is established by considering the equivalent entanglement-based scheme. In this scheme, Alice has a pure two-mode entanglement state [13]

$$|\Phi_{AB_0}\rangle = \frac{1}{2} \sum_{k=0}^3 |\psi_k\rangle_A |\alpha_k\rangle_{B_0}, \quad (1)$$

where the states

$$|\psi_k\rangle = \sum_{m=0}^3 \frac{1}{2} e^{-i(1+2k)m\pi/4} |\phi_m\rangle \quad (2)$$

are orthogonal with each other. The state $|\phi_m\rangle$ is defined as follows:

$$|\phi_m\rangle = \frac{e^{-\alpha^2/2}}{\sqrt{\xi_m}} \sum_{n=0}^{\infty} \frac{\alpha^{4n+m}}{\sqrt{(4n+m)!}} (-1)^n |4n+m\rangle, \quad (3)$$

where

$$\begin{aligned} \xi_{0,2} &= \frac{1}{2} \exp(-\alpha^2) \left(\cosh(-\alpha^2) \pm \cos(-\alpha^2) \right), \\ \xi_{1,3} &= \frac{1}{2} \exp(-\alpha^2) \left(\sinh(-\alpha^2) \pm \sin(-\alpha^2) \right). \end{aligned} \quad (4)$$

Alice holds mode A and sends mode B_0 to Bob. Then she uses a set of projection operators $|\psi_k\rangle\langle\psi_k|$ ($k = 0, 1, 2, 3$) to measure the mode she keeps. If mode A collapses into $|\psi_k\rangle$, then the mode sent to Bob collapses into $|\alpha_k\rangle$.

B. THE ENTANGLEMENT-BASED SCHEME FOR A NOISY SOURCE

When the noise in the source is taken into account, things are slightly different. In the *prepare and measure* scheme, due to the noise in the laser source and the imperfection of modulation, the state Alice sends to Bob is not a pure state $|\alpha_k\rangle$, instead it is a noisy mixed state $\rho_{B_0}^k$. Without loss of generality, let us assume that the noise on the X quadrature and the P quadrature have the same variance $\delta\varepsilon$, and their mean values are both zero. Also, we assume that the noise is induced by a neutral person Fred, and the eavesdropper Eve can not benefit from it.

In the equivalent entanglement-based scheme, as shown in Fig.1, Fred has a pure three-mode entanglement state,

$$|\Phi_{AB_0F}\rangle = \frac{1}{4} \sum_{k=0}^3 |\psi_k\rangle_A |\varphi_{B_0F}^k\rangle, \quad (5)$$

where $|\varphi_{B_0F}^k\rangle$ satisfies $\text{tr}_F(|\varphi_{B_0F}^k\rangle\langle\varphi_{B_0F}^k|) = \rho_{B_0}^k$. Fred keeps mode F and sends modes A and B_0 to Alice. Alice holds

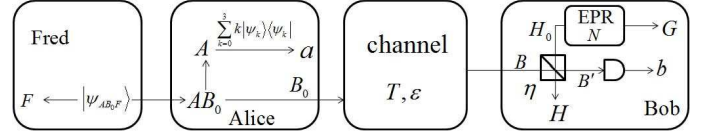


FIG. 1: The entanglement-based scheme of discretely modulated CV-QKD when considering the noise in the source. Bob uses heterodyne detection and it is assumed that Eve can not benefit from the imperfection of Bob's detector

mode A and sends mode B_0 to Bob. Then, she uses a set of projection operators $|\psi_k\rangle\langle\psi_k|$ ($k = 0, 1, 2, 3$) to measure the mode she keeps. If mode A collapses into $|\psi_k\rangle$, the mode sent to Bob collapses into $\rho_{B_0}^k$. On Bob's side, we consider the realistic model [4], in which Eve cannot benefit from the noise added by Bob's detector. In the entanglement-based scheme we can simplify the description of the realistic detector on Bob side [10]. As shown in Fig.1, the inefficiency of Bob's detector is modeled by a beam splitter with transmission η , while the electronic noise ν of Bob's detector is modeled by a thermal state ρ_{H_0} with variance N , which enters the other input port of the beam splitter. Then, Bob uses a perfect heterodyne detector to measure state $\rho_{B'}$. It is obvious to obtain that the variance of the result of Bob's measurement V_b is [17]

$$V_b = \frac{\eta}{2} V_B + \frac{1-\eta}{2} N + \frac{1}{2}, \quad (6)$$

where V_B is the variance of state ρ_B . Since the detector's efficiency is η and the electronic noise is ν , we can also obtain that

$$V_b = \eta \left(\frac{V_B}{2} + \frac{1}{2} \right) + (1-\eta) + \nu, \quad (7)$$

so we can obtain $N = 1 + 2\nu/(1-\eta)$. To consider the thermal state ρ_{H_0} as the reduced state obtained from a two-mode Gaussian state ρ_{GH_0} of variance N allows us to simplify the calculations.

C. THE OPTIMALITY OF GAUSSIAN ATTACKS FOR A NOISY SOURCE

In collective attacks, Eve uses an ancilla to interact with each pulse that Alice sends to Bob. After the interaction, the global state ρ_{AB_0F} turns into ρ_{ABEF} . On Bob's side, before his measurement, the received pulse interferes with the thermal state ρ_{H_0} , and the global state becomes $\rho_{AB'EFHG}$. Under collective attacks, when Alice and Bob use reverse reconciliation and the reconciliation efficiency is β , the secret key rate is [13]

$$K = \beta I(a : b) - \chi(b : E), \quad (8)$$

where a, b represent the classical data of Alice and Bob, $I(a : b)$ is the Shannon mutual information between a and b , and $\chi(b : E)$ is the Holevo bound, an upper bound for Eve's accessible information. When considering both the noisy source and the realistic detector, it is rather complicated

to derive the information that Eve gets by using the method introduced in Ref. [18], since the global state is an eight-mode state. So, we do not derive the secret key rate directly. Instead, we find a lower bound to K [19]

$$\tilde{K} = \beta I(a : b) - \chi(b : EF), \quad (9)$$

and $\tilde{K} \leq K$ always holds. It is obvious that when the noise in the source is small, \tilde{K} will be very close to K . Additionally, when the source is noiseless, $\tilde{K} = K$ holds. The Holevo bound $\chi(b : EF)$ is defined as

$$\chi(b : EF) = S(\rho_{EF}) - \int p(b)S(\rho_{EF}^b)db, \quad (10)$$

where $p(b)$ is the probability of the result of Bob's measurement. Before Bob's measurement, the global state is ρ_{ABEF} , so we obtain $S(\rho_{EF}) = S(\rho_{AB})$. After Bob's measurement, the global state comes into ρ_{AEFGH}^b , thus we have $S(\rho_{EF}^b) = S(\rho_{AGH}^b)$.

Notice that state $\rho_{AB'GH}$ is determined by state ρ_{AB} , so K is a function of ρ_{AB} . According to the optimality of Gaussian attacks [15, 16], for all the two-mode states ρ_{AB} with the same covariance matrix, $\tilde{K}(\rho_{AB})$ achieves the minimum value when ρ_{AB} is Gaussian. In the following, instead of K , we will derive its lower bound \tilde{K} . When the channel's transmittance is T_0 and the excess noise is ε_0 , the variance matrix of ρ_{AB} is

$$\gamma_{AB} = \begin{bmatrix} (V_A + 1)I_2 & \sqrt{T_0}Z\sigma_z \\ \sqrt{T_0}Z\sigma_z & [T_0(V_A + \varepsilon_0 + \delta\varepsilon)]I_2 \end{bmatrix}, \quad (11)$$

where $Z = 2\alpha^2 \left(\xi_0^2 \xi_1^{-\frac{1}{2}} + \xi_1^2 \xi_2^{-\frac{1}{2}} + \xi_2^2 \xi_3^{-\frac{1}{2}} + \xi_3^2 \xi_0^{-\frac{1}{2}} \right)$ reflects the correlation between mode A and mode B , $V_A = 2\alpha^2$ is just the modulation variance in the *prepare and measure* scheme, I_2 is a two-dimensional unit matrix and $\sigma_z = \text{diag}(1, -1)$. Then, we will represent the corresponding case in the Gaussian modulated protocol. In this case, Alice modulates the pure coherent states with Gaussian variables, whose variance is V_A . Then she sends them to Bob via a channel with transmittance T and excess noise ε . In the equivalent entanglement-based scheme, the variance of ρ_{AB} is

$$\gamma_{AB}^G = \begin{bmatrix} (V_A + 1)I_2 & \sqrt{T}Z_{EPR}\sigma_z \\ \sqrt{T}Z_{EPR}\sigma_z & [T(V_A + \varepsilon) + 1]I_2 \end{bmatrix}, \quad (12)$$

where $Z_{EPR} = \sqrt{V_A^2 + 2V_A}$ [13]. The entanglement states used in Gaussian-modulated CV-QKD are maximally correlated, while those in discretely modulated CV-QKD are not, so $Z < Z_{EPR}$. To make γ_{AB}^G equal to γ_{AB} , we get

$$T = T_0 \frac{Z^2}{Z_{EPR}^2}, \quad \varepsilon = \frac{Z_{EPR}^2}{Z^2} (V_A + \varepsilon_0 + \delta\varepsilon) - V_A. \quad (13)$$

According to the optimality of Gaussian attacks [15, 16], if we use discrete modulation, when the modulation variance is V_A , the variance of the noise in the source is $\delta\varepsilon$, the channel's transmittance is T_0 and excess noise is ε_0 , the lower bound of the secret key rate is just the same as the secret key rate of the case in which Alice uses Gaussian modulation with variance V_A , and the channel's transmittance and excess noise are given by Eq. (13).

D. CALCULATION OF THE SECRET KEY RATE

We call $\chi_c = 1/T - 1 + \varepsilon$ the noise added by the channel, and $\chi_d = 2(1 + \nu)/\eta - 1$ the noise induced by the heterodyne detector. Then the total noise added between Alice and Bob is

$$\chi_t = \chi_c + \chi_d/T. \quad (14)$$

When Bob uses heterodyne detection, the mutual information between Alice and Bob is [20, 21]

$$I(a : b) = \log_2 \left(\frac{V + \chi_t}{\chi_t + 1} \right), \quad (15)$$

where $V = V_A + 1$.

Then we will derive $S(\rho_{AB})$. Let $\alpha = V, \beta = T(V + \chi_c)$, and $\gamma = \sqrt{T(V^2 - 1)}$, the symplectic eigenvalues λ_1, λ_2 satisfy

$$\begin{aligned} \lambda_1^2 + \lambda_2^2 &= \alpha^2 + \beta^2 - 2\gamma^2, \\ \lambda_1^2 \lambda_2^2 &= (\alpha\beta - \gamma^2)^2. \end{aligned} \quad (16)$$

So we obtain

$$\lambda_{1,2} = \sqrt{\frac{1}{2} \left(A \pm \sqrt{A^2 - 4B} \right)}, \quad (17)$$

where $A = \alpha^2 + \beta^2 - 2\gamma^2$ and $B = (\alpha\beta - \gamma^2)^2$. Thus the entropy of ρ_{AB} is

$$S(\rho_{AB}) = g(\lambda_1) + g(\lambda_2), \quad (18)$$

where

$$g(x) = \frac{x+1}{2} \log_2 \left(\frac{x+1}{2} \right) - \frac{x-1}{2} \log_2 \left(\frac{x-1}{2} \right). \quad (19)$$

Let

$$\begin{aligned} C &= [A\chi_d^2 + 2\alpha(\alpha\beta - \gamma^2)\chi_d + 2\gamma^2 + B + 1](\beta + \chi_d)^{-2}, \\ D &= (\alpha + \sqrt{B}\chi_d)^2 (\beta + \chi_d)^{-2}, \end{aligned} \quad (20)$$

then the entropy of ρ_{AGH}^b is [21]

$$S(\rho_{AGH}^b) = g(\lambda_3) + g(\lambda_4), \quad (21)$$

where

$$\lambda_{3,4} = \sqrt{\frac{1}{2} \left(C \pm \sqrt{C^2 - 4D} \right)}. \quad (22)$$

Since $S(\rho_{AGH}^b)$ is independent of Bob's measurement b , we obtain

$$\int p(b)S(\rho_{AGH}^b)db = S(\rho_{AGH}^{b_0}), \quad (23)$$

where b_0 is a constant.

So, in the discretely modulated CV-QKD, the lower bound to the secret key rate is

$$\tilde{K} = \beta \log_2 \left(\frac{V + \chi_t}{\chi_t + 1} \right) - g(\lambda_1) - g(\lambda_2) + g(\lambda_3) + g(\lambda_4). \quad (24)$$

It is enough to derive the lower bound of the secret key rate against collective attacks, because they are proven to be the most powerful attacks in the asymptotic limit [22, 23].

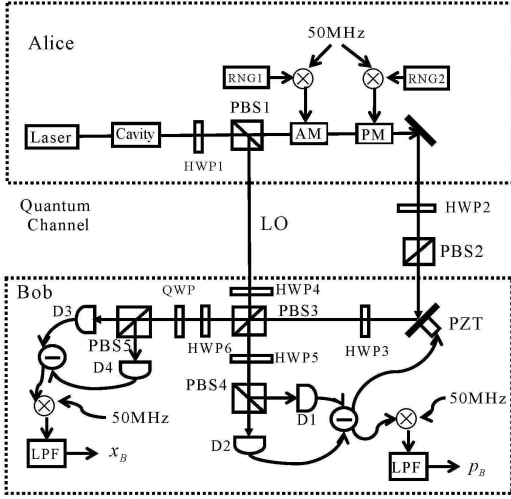


FIG. 2: The experimental schematic of discretely modulated CV-QKD. Laser, NP Photonics (1550 nm); RNG1,-2, random number generators; HWP1C6, half-wave plates; PBS1C5, polarizers; PZT, piezoelectric transducer; QWP, quarter-wave plate; DIC4, detectors; LPF, low-pass filter.

III. IMPLEMENTATION OF DISCRETELY MODULATED CV-QKD

A. EXPERIMENTAL SETUP

The schematic of our experimental setup is shown in Fig. 2. The laser source is a 1550-nm continuous-wave fiber laser (NP Photonics). The noise in the laser has been mainly suppressed by a mode cleaner, which is a triangle resonant cavity with a finesse of 500. Alice uses HWP1 and PBS1 to split a small part of the light as the signal, and the rest as the LO. The signal's power is about $4\mu\text{W}$, and the LO's power is 40mW in our experiment. Then, Alice mixes two random electronic signals with a 50-MHz carrier, and sends the outputs of the mixers to amplitude and phase modulators to modulate the signal. Alice generates binary pseudorandom numbers by using a programmable function generator (Agilent33250A) in our experiment. Since the generation rate of random electronic signals on Alice's side is 10MHz, the width of each coherent state is 100ns. The LO and the signal are sent to Bob through the quantum channel. We use HWP2 and PBS2 to replace the lossy channel (no excess noise).

When Bob receives the signal that Alice sends, he splits it into two beams with HWP3 and PBS3. At one of the output ports of PBS3, he makes a homodyne detection and uses the DC part of the result as a feedback signal to control the PZT, so as to lock the relative phase between the signal and the LO at $\pi/2$. So, he is actually measuring the P quadrature at this port. At the other output port, he uses QWP to induce a $\pi/2$ phase shift between the signal and the LO, and he makes a homodyne detection to measure the X quadrature. We design a broadband balanced detector with a photodiode G8376-05 by Hamamatsu. The effective bandwidth is over 100 MHz, and the SNR is near 9.2 dB for 20-mW coherent light as shown

in Fig. 3. The outputs of detectors are mixed with a 50-MHz carrier and filtered by 25-MHz LPFs. The outputs of filters are sampled by a data acquisition card NI PXIe-5122, and the sampling rate is 50 MHz.

B. MODULATION AND NOISE SUPPRESSION

In our experiment, the signal is not a weak coherent state but has a large offset. When the signal and the LO's phase is locked, the initial state can be written as $|x_0\rangle$, while the modulated state can be written as $|x_0 + x + ip\rangle$, where x and p are the signals added to the X and P quadratures of the light respectively. If $x, p \ll x_0$, amplitude A and phase θ of the modulated light are

$$\begin{aligned} A &= \sqrt{(x_0 + x)^2 + p^2} \approx x_0 + x, \\ \theta &= \arctan(p/(x + x_0)) \approx p/x_0. \end{aligned} \quad (25)$$

So, when Alice modulates the amplitude and the phase of the light, she is just modulating the X and P quadratures of the light, respectively. The half-wave voltage of the amplitude and the phase modulators is 360V, while the electronic signals Alice adds to them are less than 2 V, so the condition $x, p \ll x_0$ is satisfied.

The light generated by the fiber laser, which has much relative intensity noise and phase noise in our experiment, can be treated as a coherent state whose amplitude and phase are randomly modulated. It is not a pure state but a mixed state and can be written as $\rho = \int P(n_A, n_P) |\alpha(n_A, n_P)\rangle \langle \alpha(n_A, n_P)| dn_A dn_P$, where $|\alpha(n_A, n_P)\rangle = |(x_0 + n_A) e^{in_P}\rangle$. This can be regarded as the fact that the source generates a pure state $|\alpha(n_A, n_P)\rangle$ with the probability $P(n_A, n_P)$. So for a particular state, we treat it as a coherent state $|\alpha(n_A, n_P)\rangle$, but the parameters n_A and n_P are unknown. When Alice modulates its amplitude and phase by x and p/x_0 , respectively, it becomes $|(x_0 + n_A + x) e^{i(n_P + p/x_0)}\rangle$ and can be written as $|(x_0 + n_A + x + ip) e^{in_P}\rangle$ when $x, p \ll x_0$. The LO can be written as $|\alpha_{LO} e^{i(\varphi + n_P)}\rangle$, where α_{LO} is a real number, α_{LO}^2 is the intensity of the LO, and φ is the phase shift added by Bob. The LO is quite strong, so its amplitude noise can be ignored, and it has the same phase noise n_P with the signal when their optical path difference is far less than the coherence length, since they come from one beam. In homodyne detection, the difference of photoelectrons generated by two photodiodes satisfies [20]

$$\Delta N_e \propto \alpha_{LO} (\cos \varphi \hat{x} + \sin \varphi \hat{p}). \quad (26)$$

From Eq. (26), we can see that the phase noise in the laser source has no effect on the results of the P quadrature measurement, since the phase noise n_P does not appear in Eq. (26). This is consistent with our experimental results. Whether the mode cleaner is added or not, the noise on the P quadrature can reach the shot-noise limit. However, matters are quite different with the X quadrature. When we measure the noise of the X quadrature without the mode cleaner, there is a very sizable classical noise with a sideband frequency up

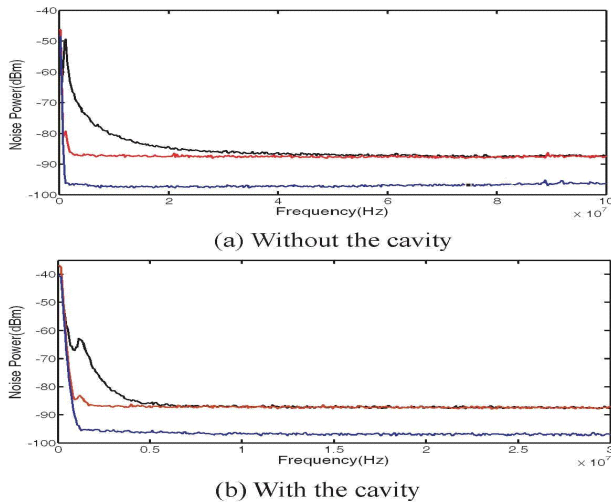


FIG. 3: (Color online) (a) The noise spectrum (0-100 MHz) of the X quadrature measurement of the signal without cavity (the highest curve), shot noise (the middle curve), and electronics noise (the lowest curve). (b) The noise spectrum (0-30 MHz) of the X quadrature measurement of the signal with cavity (the highest curve), shot noise (the middle curve), and electronics noise (the lowest curve).

to 50 MHz, as shown in Fig. 3(a). So, Alice uses a mode cleaner to purify the noisy coherent state. After purification, the amplitude noise above 10 MHz is remarkably suppressed and almost reaches the shot-noise limit, as shown in Fig. 3(b).

Although the high-frequency noise above 10 MHz has been suppressed, there is still much residual low-frequency noise under 10 MHz. In order to avoid this noise, Alice uses two strings of random numbers that she wants to send to mix with a 50-MHz carrier. Then, she modulates the two mixed electronic signals to the amplitude and phase modulators, respectively. Bob can filter the low frequency noise easily and can pick up the interested frequency component by using a mixer and an LPF. Finally, the noise in the source is suppressed to the shot-noise limit and can be neglected. The relative phase between the signal and the LO is locked, so the phase noise of the interferometer is small enough to be ignored. In Gaussian-modulation-based protocols, the modulation variance is large, so it will induce notable excess noise [9]. However, in our experiment, the modulation variance is quite small (see the following), and the noise caused by the imperfect modulation can be ignored.

C. DATA PROCESSING

In order to get the measurement results of X and P quadratures of the n th coherent state, Bob needs to get the n th difference of photoelectrons ΔN_{en} . Since the width of each coherent state is $T = 100ns$, we obtain

$$\Delta N_{en} \propto \int_{(n-1)T}^{nT} V(t)dt, \quad (27)$$

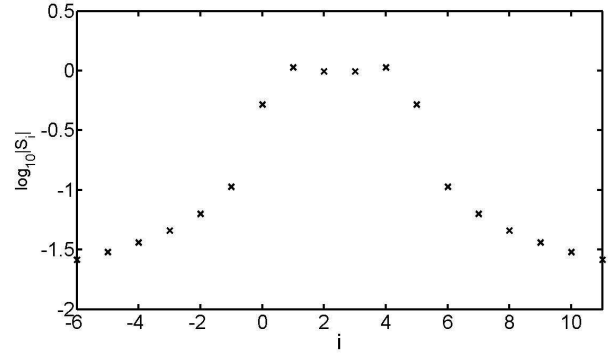


FIG. 4: $\log_{10} |S_i|$ as a function of i .

where $V(t)$ is the output of the LPF. In practice, Bob does not integrate $V(t)$, instead he samples it at $t_i = i\tau$ and gets V_i ($i = 0, 1, 2, \dots$), where $\tau = 20ns$ is the sampling interval, and V_i is the sampling value. The bandwidth of $V(t)$ is less than 25MHz, so Bob can get all of the information of $V(t)$ with the sampling rate of 50MHz. Bob can rebuild $V(t)$ with his samples [24]

$$V(t) = \sum_{i=-\infty}^{\infty} V_i \text{sinc}\left(\frac{t}{\tau} - i\right), \quad (28)$$

so

$$\begin{aligned} \Delta N_{en} &\propto \int_{5(n-1)\tau}^{5n\tau} \sum_{i=-\infty}^{\infty} V_i \text{sinc}\left(\frac{t}{\tau} - i\right) dt \\ &= \sum_{i=-\infty}^{\infty} V_i \int_{(5n-i-5)\tau}^{(5n-i)\tau} \text{sinc}\left(\frac{t}{\tau}\right) dt = \sum_{i=-\infty}^{\infty} V_i S_{i-5n+5}, \end{aligned} \quad (29)$$

where $S_i = \int_{-i\tau}^{(5-i)\tau} \text{sinc}(t/\tau)dt$ is symmetric with $i = 2.5$. By considering that the absolute value of S_i attenuates quickly with the absolute value of $i - 2.5$, as shown in Fig. 4, in practice, the sum in Eq. (29) is truncated from $i = 0$ to $i = 5$. So, the measurement result of the n th coherent state (take the X quadrature for instance) is

$$X_n \approx k \sum_{i=0}^5 V_{5n+i-5} S_i, \quad (30)$$

where the constant k contains all the dimensional prefactors.

Thus, Bob approximately obtains the total difference of photoelectrons when he measures the received signal with this method. If Eve attacks by measuring the signal during time windows which are not sampled by Bob, she can not do it without being discovered, because she will inevitably the total difference of photoelectrons obtained by Bob. Actually, if Eve uses this attack, she will increase the loss observed by Bob. So, the proposed protocol is secure against this attack.

D. EXPERIMENTAL RESULT AND DISCUSSION

The homodyne detectors are carefully calibrated, and their efficiencies are both $\eta = 0.8$. Then we need to determine the

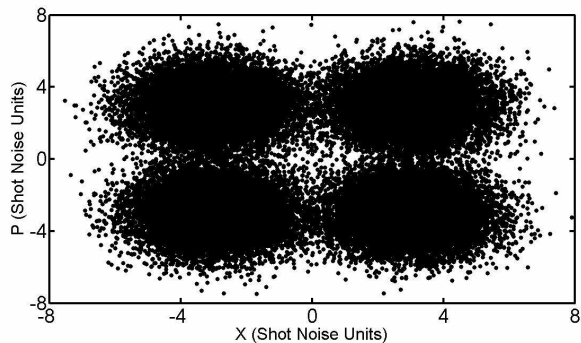


FIG. 5: The result of Bob's heterodyne measurement when the modulation variance is 18.

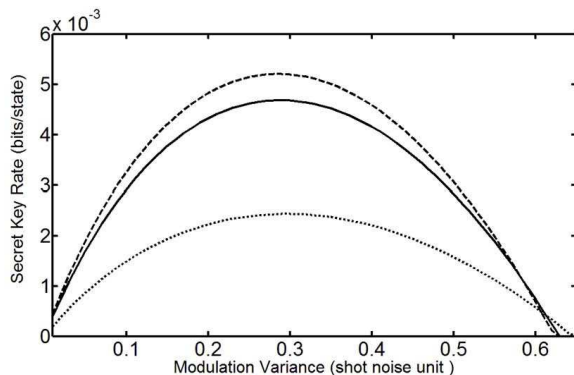


FIG. 6: The secret key rate as a function of the modulation variance for an electronic noise of 0.12 (solid line), 0 (dashed line), and 1.2 (dotted line). The channel is noiseless, and its transmittance is 0.1; the efficiency of the detector is 0.8, and the reconciliation efficiency is 0.8.

excess noise in Bob's homodyne detector. We just simulate the channel loss by using a beam splitter on a tabletop, so the channel's excess noise ε is 0. When the channel's transmittance is $T = 1$ and the modulation variance is 18, the result Bob gets is shown in Fig. 5. There are 50000 points in this figure. From the data, we can calculate the excess noise in the detectors. The total added noise is determined experimentally to be about $\chi_t = 1.8$. Since $T = 1$, $\varepsilon = 0$ and $\eta = 0.8$, from Eq. (14) we obtain $\nu = 0.12$. According to Eq. (2), we can find the maximal secret key rate by scanning the modulation variance V_a , as shown in Fig. 6. As a result, for a 90% lossy channel and the reconciliation efficiency of 80%, when the modulation variance is 0.29, we achieve the maximal secret key rate of 46.8 kbits/s at the encoding rate of 10 MHz.

We can also see that even if the electronic noise is suppressed at 0, the optimal secret key rate per coherent state is just 5.02×10^{-3} bits, which is only a little bit higher than that in our experiment. So, it is not very wise to enhance the secret

key rate by suppressing the electronic noise of the detectors.

In our experiment, the encoding rate is limited by the bandwidth of the detectors, which is 100M. The secret key rate can be further enhanced by increasing the encoding rate, which needs a broader bandwidth detector and will lead to higher electronic noise. For detectors with a certain gain-bandwidth product, if we broaden the bandwidth B to $\sqrt{10}B$, the gain G becomes $10^{-0.5}G$, which leads to a electronic noise of 1.2. In this case, the optimal secret key rate is 2.43×10^{-3} bits/state, and the secret key rate per second is 1.64 times as before. So, we can enhance the secret key rate by decreasing the gain of the detectors so as to broaden their bandwidth and to increase the encoding rate.

IV. CONCLUSION

In this paper, we derive a lower bound to the secret key rate when considering the noise in the source, and we present a discretely modulated CV-QKD system by using strong coherent states and heterodyne detection. We assume that the noise in the source is induced by a neutral person Fred, and we present the equivalent entanglement-based scheme. In this scheme, Eve can not purify the state shared by Alice and Bob, so we can not calculate the secret key rate. Instead, we derive a lower bound for the secret key rate. In our experiment, the noise of the laser is suppressed at the shot-noise limit by using a cavity and the method of frequency shift. Since the modulation variance is quite small and the relative phase between the signal and the LO is locked to perform heterodyne detection, the excess noise induced by the imperfection of modulation and the phase noise in the interferometer is negligible. In order to increase the repetition rate, we broaden the bandwidth of the detector at the expense of low SNR. When the channel loss is 90%, we achieve a secret key rate of 46.8 kbits/s with the optimal modulation variance and the encoding rate of 10 MHz. For detectors with a certain gain-bandwidth product, the secret key rate can further be improved by broadening the bandwidth of detectors and by increasing the encoding rate. However, the secret key rate is only an estimation and is not a real one. Many actions must be conducted, such as error correction, privacy amplification, and reduction of guided acoustic-wave Brillouin scattering in fiber-optic implementations, which are what we will perform in a future work.

V. ACKNOWLEDGMENTS

The authors thank Hong Guo's group for useful discussions. The work is supported by the key project of the Preparatory Research Foundation of the National University of Defense Technology (Grant No. JC08-02-01) and the National Natural Science Foundation of China (Grant No. 10904174).

[1] F. Grosshans and P. Grangier, Phys. Rev. Lett. **88**, 057902 (2002).

[2] C. H. Bennett, G.Brassard, Proceedings of *IEEE International*

- Conference on Computers, Systems, and Signal Processing* (IEEE, New York, 1984), pp. 175-179 (1984).
- [3] F. Grosshans and P. Grangier, E-print arXiv:quant-ph/0204127 (2002).
- [4] F. Grosshans, G. Van Assche, J. Wenger, R. Tualle-Brouri, N. J. Cerf, and P. Grangier, *Nature (London)* **421**, 238 (2003).
- [5] Ch. Silberhorn, T. C. Ralph, N. Lutkenhaus, and G. Leuchs, *Phys. Rev. Lett.* **89**, 167901 (2002).
- [6] C. Weedbrook, A. M. Lance, W. P. Bowen, T. Symul, T. C. Ralph, and P. K. Lam, *Phys. Rev. Lett.* **93**, 170504 (2004).
- [7] A. M. Lance, T. Symul, V. Sharma, C. Weedbrook, T. C. Ralph, and P. K. Lam, *Phys. Rev. Lett.* **95**, 180503 (2005).
- [8] T. Symul, D. J. Alton, S. M. Assad, A. M. Lance, C. Weedbrook, T. C. Ralph, and P. K. Lam, *Phys. Rev. A* **76**, 030303(R) (2007).
- [9] J. Lodewyck, T. Debuisschert, R. Tualle-Brouri, and P. Grangier, *Phys. Rev. A* **72**, 050303(R) (2005).
- [10] J. Lodewyck, M. Bloch, R. García-Patrón, S. Fossier, E. Karpov, E. Diamanti, T. Debuisschert, N. J. Cerf, R. Tualle-Brouri, S. W. McLaughlin, and P. Grangier, *Phys. Rev. A* **76**, 042305 (2007).
- [11] B. Qi, L. L. Huang, L. Qian, and H. K. Lo, *Phys. Rev. A* **76**, 052323 (2007).
- [12] Z. Zhang and P. L. Voss, *Opt. Exp.* **17** 12090 (2009).
- [13] A. Leverrier and P. Grangier, *Phys. Rev. Lett.* **102** 180504 (2009).
- [14] Q. D. Xuan, Z. Zhang, and P. L. Voss, *Opt. Exp.* **17**, 24244 (2009).
- [15] M. Navascués, F. Grosshans, and A. Acín, *Phys. Rev. Lett.* **97**, 190502 (2006).
- [16] R. Garcia-Patron and N. J. Cerf, *Phys. Rev. Lett.* **97**, 190503(2006).
- [17] F. Grosshans and N. J. Cerf, *Quantum Inf. Comput.* **3**, 535 (2003).
- [18] V. C. Usenko and Radim Filip, *Phys. Rev. A* **81** 022318 (2010).
- [19] Y. Shen, J. Yang, and H. Guo, *J. Phys. B* **42** 235506 (2009).
- [20] R. Garcia-Patron Ph. D. thesis, Universite Libre de Bruxelles, Bruxelles 2007 (unpublished).
- [21] S Fossier, E Diamanti, T Debuisschert, R Tualle-Brouri, and P Grangier *J. Phys. B* **42** 114014 (2009).
- [22] R. Renner, J. I. Cirac, *Phys. Rev. Lett.* **102**, 110504 (2009).
- [23] A. Leverrier, E. Karpov, P. Grangier, N. J. Cerf, *New J. Phys.* **11** 115009 (2009) .
- [24] C. E. Shannon, *Proc. IRE*, **37**, 10 (1949).